Mechanics & Industry 13, 317–323 (2012)
© AFM, EDP Sciences 2012
DOI: 10.1051/meca/2012028
www.mechanics-industry.org

Mechanics & Industry

A windage power loss model based on CFD study about the volumetric flow rate expelled by spur gears

Sylvain Pallas[1], Yann Marchesse[1,a], Christophe Changenet[1], Fabrice Ville[2] and Philippe Velex[2]

[1] Université de Lyon, ECAM Lyon, Laboratoire d'Énergétique, 40 montée Saint-Barthélemy, 69005 Lyon, France
[2] Université de Lyon, CNRS, INSA-Lyon, LaMCoS UMR 5259, 18–20 rue des Sciences, 69621 Villeurbanne, France

Received 1 February 2012, Accepted 25 September 2012

Abstract – This paper investigates the windage power losses generated by spur gears rotating in pure air by using a computational fluid dynamics (CFD) code. The three-dimensional simulations are at first validated comparing CFD predictions with the power losses measured in similar conditions from other investigations. The volumetric flow rate which is expelled by the teeth is then analysed, and a correlation which is based on a classical approach used in turbomachinery is finally proposed which makes it possible to estimate windage losses for spur gears. It was observed that this latter approach seems satisfying since the formulation of the volumetric flow rate which is employed in the model is appropriate to each gear.

Key words: Spur gears / windage power loss / CFD / correlation

Résumé – Modèle des pertes par ventilation basé sur une étude numérique du débit d'air éjecté par une denture droite d'engrenage. Cette étude s'intéresse aux pertes par ventilation observées dans le cas d'engrenages droits et estimées à l'aide d'un code de calcul classique. L'approche numérique est d'une part validée par comparaison des prévisions numériques des pertes avec celles mesurées dans des conditions similaires. Les débits éjectés par la périphérie des roues dentées sont ensuite analysés, et un modèle capable d'estimer les pertes par ventilation et basé sur une analogie avec la cinématique de l'écoulement dans un système rotor est d'autre part proposé. Ce modèle semble adapté à l'estimation des pertes tant que le modèle du débit éjecté reste en rapport des roues dentées étudiées.

Mots clés : Denture droite / pertes par ventilation / CFD / modèle

1 Introduction

Numerous experiments have demonstrated that no-load power losses and windage in particular, become prominent when considering high speed gear transmissions. Anderson et al. [1] and Townsend [2] proposed empirical formulations for the estimation of windage power losses (WPL) including face width and pitch radius whereas Dawson [3,4] employed the module values in addition with the two previous parameters. Diab et al. [5] focused on the air circulation around the gear involving an active surface located on teeth contributing to the fluid ejection. More recently a physics-based fluid mechanics model has been proposed which includes both windage and churning losses (Seetharaman and Kahraman [6]). However when a single rotating spur gear is considered none of these models clearly consider the influence of the tooth geometrical dimensions other than the module and addendum characteristics. In an effort to analyze single phase flows around spur gears (Al-Shibl et al. [7]) or bevel gears (Rapley et al. [8]), different approaches have been proposed which rely on computational fluid dynamics (CFD) codes. For spur gears, two-dimensional CFD models have been used which reveal that the air flow is trapped within the inter-tooth spaces in accordance with the hypotheses used in [7]. However, these findings are quite different from those which are based on three-dimensional CFD models. Hence Hill et al. [9] adapted an unstructured overset moving mesh CFD method on entire unshrouded, isolated, rotating, spur gears in order to investigate WPL for a rotorcraft gearbox. The authors concluded that the air flow was highly three-dimensional in nature and demonstrated that the air expelled in the radial direction from the inter-tooth zone played an important role in the power loss mechanism.

[a] Corresponding author: yann.marchesse@ecam.fr

Article published by EDP Sciences

https://doi.org/10.1051/meca/2012028 Published online by Cambridge University Press

Nomenclature

b	tooth face width (m)
h	tooth depth (m)
k	turbulent kinetic energy ($m^2.s^{-2}$)
Q	volumetric flow rate ($m^3.s^{-1}$)
R	pitch radius (m)
r	radius (m)
S	section area (m^2)
t	time (s)
U	peripheral velocity ($m.s^{-1}$)
u_i	velocity component ($m.s^{-1}$)
u_τ	wall friction velocity ($m.s^{-1}$)
V	absolute velocity ($m.s^{-1}$)
W	relative velocity ($m.s^{-1}$)
x_i	Cartesian coordinate (m)
y	distance from the wall in $y+$ formulation (m)
$y+$	dimensionless distance from wall parameter
Z	number of teeth
γ	angle (rad)
λ	volumetric flow rate coefficient (m)
δ_{ij}	Kronecker's symbol
ε	turbulent dissipation rate ($m^2.s^{-3}$)
μ	dynamic viscosity (Pa.s)
μ_t	eddy viscosity (Pa.s)
ρ	fluid density ($kg.m^{-3}$)
$\rho\overline{u_i'u_j'}$	Reynolds stress (Pa)
τ	external force moments (N.m)
τ_w	wall shear stress (Pa)
ω	specific dissipation rate (s^{-1})
Ω	angular velocity ($rad.s^{-1}$)
Subscripts	
1	inlet
2	outlet
r	radial component
u	tangential component

Marchesse et al. [10] used a structured mesh of a single-gear tooth, with periodic boundary conditions, in a rotating reference frame. This simplified approach led to similar results as Hill et al. [9] and it is shown that WPL are closely linked with the associated expelled volumetric flow rate and finally the tooth geometry. This latter point has been confirmed recently in Reference [11] as a variation of both expelled volumetric flow rate and WPL is noticed when a modification of dedendum parameter is made. The complex link between WPL, expelled volumetric flow rate, and gear tooth geometry has to be investigated if more adapted correlations are needed. In that way this study aims at investigating at first the volumetric flow rate expelled by three spur gears (Tab. 1). The purpose is then to propose a correlation of WPL involving tooth geometry.

This paper is organized as follows. First the numerical approach is introduced. Comparisons between WPL predicted numerically and experimental data which have been obtained in similar conditions are then performed which validate the numerical approach. The volumetric flow rate is analyzed in order to develop an analytical formulation of this parameter. Finally a formulation, based on a classical approach used in turbomachinery, is proposed which makes it possible to estimate windage losses for spur gears.

2 Numerical approach

The configuration to be studied here is presented in Figure 1. The computational domain comprises one single tooth, the associated fraction of the blank, and the surrounding air.

The airflow is supposed to be governed by incompressible Navier-Stokes equations since the maximum local Mach number was found to be less than 0.3. Numerical local solutions are obtained using commercial software ANSYS-CFX 12.1 based on the Reynolds-Averaged Navier-Stokes (RANS) theory [12]. The finite volume discretization method approximates the differential equations by a system of algebraic equations for the variables at some set of discrete locations in space. The averaged continuity and momentum equations for an incompressible viscous flow without body force read:

$$\frac{\partial\left(\rho\overline{u_i}\right)}{\partial x_i}=0, \tag{1}$$

$$\frac{\partial\left(\rho\overline{u_i}\right)}{\partial t}+\frac{\partial}{\partial x_j}\left(\rho\overline{u_i}\,\overline{u_j}+\rho\overline{u_i'u_j'}\right)=-\frac{\partial\overline{p}}{\partial x_i}+\frac{\partial}{\partial x_j}\left[\mu\left(\frac{\partial\overline{u_i}}{\partial x_j}+\frac{\partial\overline{u_j}}{\partial x_i}\right)\right] \tag{2}$$

No simplifications of these governing RANS equations are possible here since there is no dominant mean-flow direction. The Reynolds stresses $\rho\overline{u_i'u_j'}$ must be modelled in order to close the latter equations. This is generally achieved using the eddy-viscosity hypothesis:

$$-\rho\overline{u_i'u_j'}=\mu_t\left(\frac{\partial\overline{u_i}}{\partial x_j}+\frac{\partial\overline{u_j}}{\partial x_i}\right)-\frac{2}{3}\rho\delta_{ij}k \tag{3}$$

where k is the turbulent kinetic energy, and μ_t stands for the eddy viscosity. To reach an appropriate numerical approach, closure is here shear stress transport (SST) k-ω model [13], where ε is the rate of dissipation and ω is the specific dissipation rate: $\omega=\varepsilon/(C_\mu k)$. In this model, the eddy viscosity is computed by combining k and ω as follows:

$$\mu_t=\alpha\frac{\rho k}{\omega} \tag{4}$$

The turbulence kinetic energy and the specific dissipation rate are obtained from the following transport equations:

$$\frac{\partial}{\partial t}\left(\rho k\right)+\frac{\partial}{\partial x_i}\left(\rho k u_i\right)=\frac{\partial}{\partial x_j}\left[\Gamma_k\frac{\partial k}{\partial x_j}\right]-\rho\overline{u_i'u_j'}\frac{\partial u_j}{\partial x_i}-Y_k \tag{5}$$

and

$$\frac{\partial}{\partial t}\left(\rho\omega\right)+\frac{\partial}{\partial x_i}\left(\rho\omega u_i\right)=\frac{\partial}{\partial x_j}\left[\Gamma_\omega\frac{\partial\omega}{\partial x_j}\right]-\alpha\frac{\omega}{k}\rho\overline{u_i'u_j'}\frac{\partial u_j}{\partial x_i}-Y_\omega \tag{6}$$

https://doi.org/10.1051/meca/2012028 Published online by Cambridge University Press

Table 1. Gear characteristics.

Gear #	Pitch diameter (mm)	Module (mm)	Face width (mm)	Pressure angle (°)
1	100	5	24	20
2	150	5	24	20
3	288	4	30	20

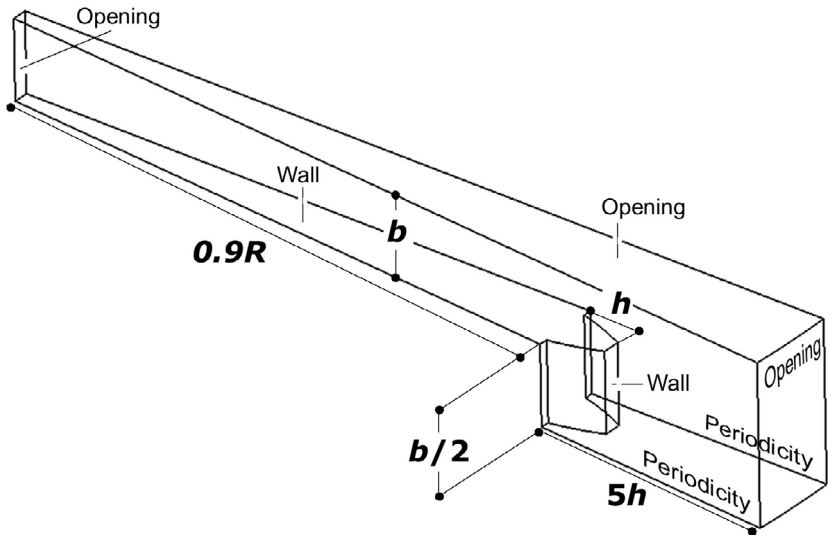


Fig. 1. Schematic of 3D computation domain and boundary conditions imposed at external surfaces.

where Γ_k and Γ_ω represent the effective diffusivity of k and ω; Y_k and Y_ω characterise the dissipation of k and ω due to the turbulence. The strategy of using SST k-ω model lies on the fact that it has been shown yet [9,10] that using a high-Reynolds number turbulent model (e.g. standard k–ε) leads to underestimation of WPL. The equations are solved on structured grids with strong clustering close to the walls in order to capture the near-wall turbulent region. For that the dimensionless wall parameter $y+$ which is defined by $y+ = \rho y u_\tau/\mu$ is less than 3. In this relation y is the distance from the centre of the first cells to the wall and u_τ is the wall friction velocity given by $u_\tau = \sqrt{|\tau_w|/\rho}$ where τ_w is the shear stress at the wall. The value of $y+$ is sufficiently low so that the first grid points are located in the laminar part of the boundary layer. This location is in good agreement with the use of the SST k-ω model.

The boundary conditions which are imposed at external surfaces are presented in Figure 1. For all the computations, a nil velocity is imposed at all the nodes located on the gear tooth surfaces. Periodic conditions are applied to the two surfaces where the fluxes of all variables are supposed to be identical. The normal velocity component at the planes of symmetry is set to zero and an opening condition is imposed to the other external surfaces. Rotational speeds between 100 and 700 rad.s^{-1} are considered. The surrounding fluid is supposed to be pure air, the physical properties of which are evaluated at 25 °C (e.g. $\rho = 1.185$ kg.m^{-3} and $\mu = 1.831 \times 10^{-5}$ Pa.s). Convergence is reached when both the equation residuals are low and the drag torque caused by windage keeps constant amplitude.

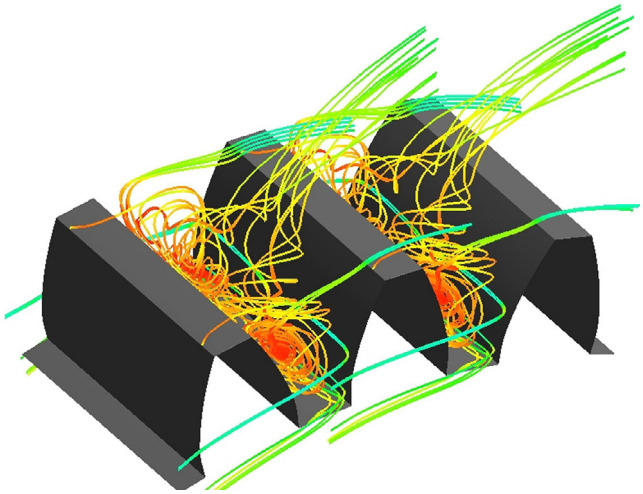


Fig. 2. Flow pattern (gear #3 at 700 rad.s^{-1}).

3 Numerical results

The numerical predictions exhibit a complex flow pattern independent of gear geometry and speed: the air from the gear side is drawn axially, circulation then takes place over the entire volume and, finally, the flow is expelled by centrifugal effects (Fig. 2). One part of the expelled air also comes from the region above the tip tooth radius. The flow pattern seems then similar with the trajectory of fluid in centrifugal rotor system. The comparison between numerical predictions and experimental data of WPL is satisfying as relative error deviation reaches only 11 percent at maximum for gear #3 at 700 rad.s^{-1} (Fig. 3). The

https://doi.org/10.1051/meca/2012028 Published online by Cambridge University Press

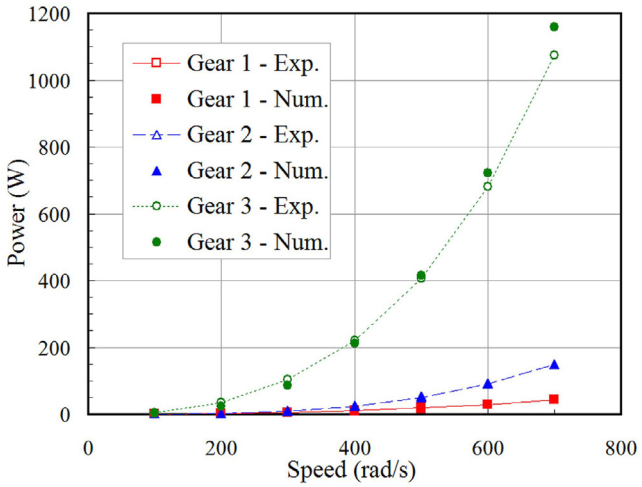


Fig. 3. Experimental and numerical windage power losses.

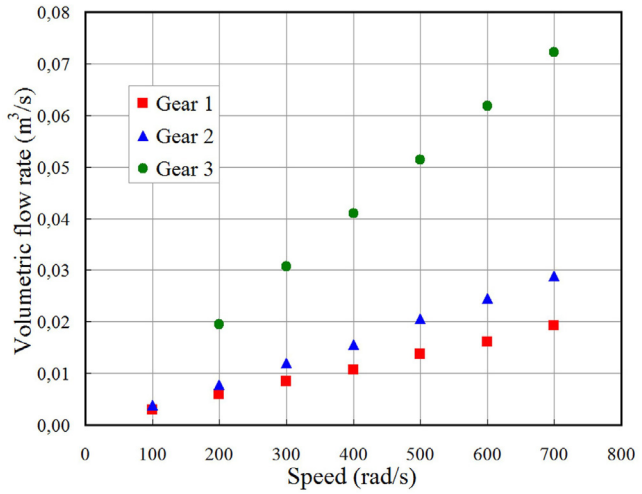


Fig. 4. Volumetric flow rate expelled by the entire gears.

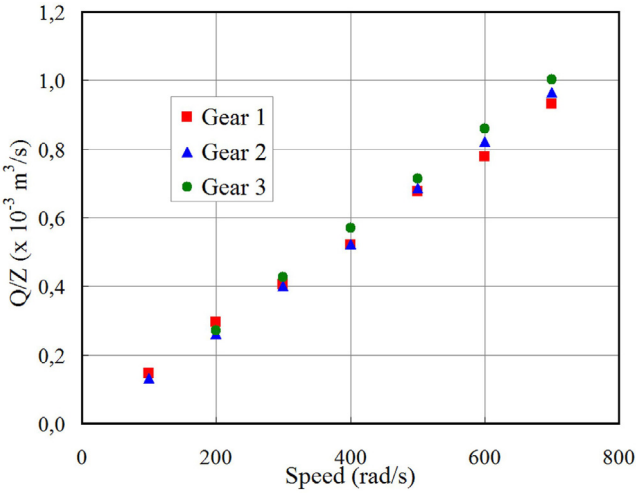


Fig. 5. Volumetric flow rate expelled per unit of teeth.

numerical approach used here is then validated. One notices also that the dissipation due to friction is negligible since it represents at maximum 11% of the total windage power losses when using gear #3 rotating at 700 rad.s^{-1}.

Moreover it is found that the volumetric flow rate passing through the intertooth spaces varies almost linearly with both the rotational speed (Fig. 4) and the number of teeth (Fig. 5). However the volumetric flow rate is slightly influenced by the pitch diameter: increasing the latter parameter (gears #1, #2, and #3) generates a few more airflow rate.

4 Analytical models

4.1 Volumetric flow rate

From the observations above, the expelled volumetric flow rate may be written in a first approximation as proportional to both the rotational speed and the number of teeth. The tooth height contribution must also be added since it has been shown in a previous study [11] that the volumetric flow rate varies with its values. Moreover it has been above-mentioned that the volumetric flow rates expelled by one tooth are almost similar whatever the studied gears are, despite the difference between the values of module and face width parameters (Fig. 5, Tab. 1). Hence face width value for gear #3 is 25% higher than those observed for gears #1 and #2. This increasing is however balanced by a decrease in tooth height *via* module quantity since the value noticed for gear #3 is 20% lower than the ones characterising gears #1 and #2. Contribution of the product bh, where b and h are respectively face width and tooth height, must be then considered in the volumetric flow rate model instead of h alone. Finally the model which is able to predict expelled volumetric flow rate reads:

$$\mathrm{Q}_{\mathrm{Mod.}} = \lambda \times Z \times h \times \mathrm{b} \times \Omega \tag{7}$$

where Z is the number of teeth and Ω is the angular velocity. λ is a coefficient which can be determined from the numerical predictions of volumetric flow rate and geometrical data for the three studied gears. It appears that constant values are reached whatever the gears considered for rotational speed greater than 400 rad.s^{-1} (Fig. 6). However while λ nearly equals to 5.07×10^{-3} m and 5.05×10^{-3} m respectively for gears #1 and #2, the estimation is slightly higher for gear #3 (i.e. $\lambda = 5.30 \times 10^{-3}$ m) which is in accordance with previous observations.

Using values of λ, obtained for each gear when the rotational speed is greater than 400 rad.s^{-1}, in relation (7), a good agreement is noticed between predictions of volumetric flow rate from the model and from the numerical part (Fig. 7a). Moreover, considering angular velocities higher than 400 rad.s^{-1}, the maximum relative error equals 1.8% for gear #1 rotating at 600 rad.s^{-1}. More important relative-errors are observed when the mean value of volumetric flow rate coefficient, i.e. $\overline{\lambda} = 5.11 \times 10^{-3}$ m, is employed this time in (7). Thus, the volumetric flow

https://doi.org/10.1051/meca/2012028 Published online by Cambridge University Press

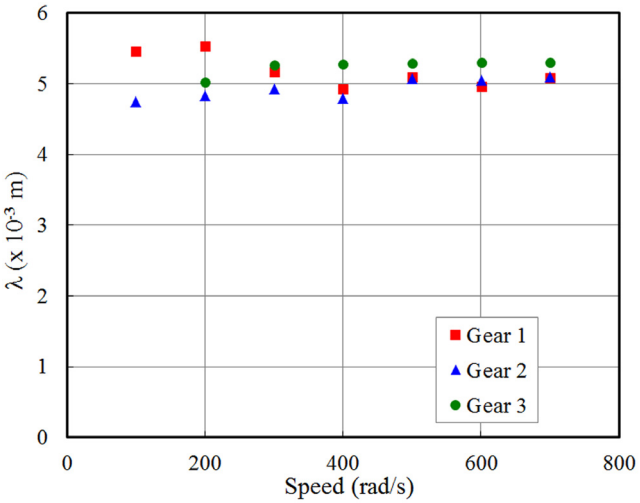


Fig. 6. Evaluation of volumetric flow rate coefficient.

rate predicted by the model for gear #3 is slightly underestimated (Fig. 7b). However the relative-errors between numerical data and values from the model never exceed 3.1% for this latter gear.

4.2 Windage power losses

Solutions in the previous section reveal that gears rotating in a fluid present similarities with centrifugal streamlines as indicated by the volumetric flow rate evolution with rotational speed. It seems therefore interesting to explore the possibility of an analytical approach to WPL using some well-known results in turbomachinery analysis [14].

Considering the control volume enclosing the rotating gear, it is supposed that air enters the control volume at radius r_1 (root radius) with an absolute velocity V_1 and leaves it at radius r_2 (tip radius) with an absolute velocity V_2. As shown in Figure 8, the absolute velocity is decomposed into the relative velocity parallel to the tooth surface (W) and the tooth peripheral velocity (U). Alternatively, the absolute velocity can also be split into the sum of a radial (V_r = velocity of flow) and tangential component (V_u = velocity of whirl). For a gear running with angular velocity Ω, the specific work generated on the fluid (work per unit of mass) is given by [14]:

$$\frac{\tau\,\Omega}{\rho Q} = U_2\,V_{u2} - U_1\,V_{u1} \tag{8}$$

where $U = \Omega r$; τ represents the sum of the moments of the external forces acting on the fluid in the control volume. Neglecting the dissipation by friction (which is justified in previous section), the product $\tau\Omega$ corresponds to the WPL. Since the fluid enters the control volume mostly in the axial direction, the inlet tangential velocity can be neglected and the fluid outlet tangential and radial

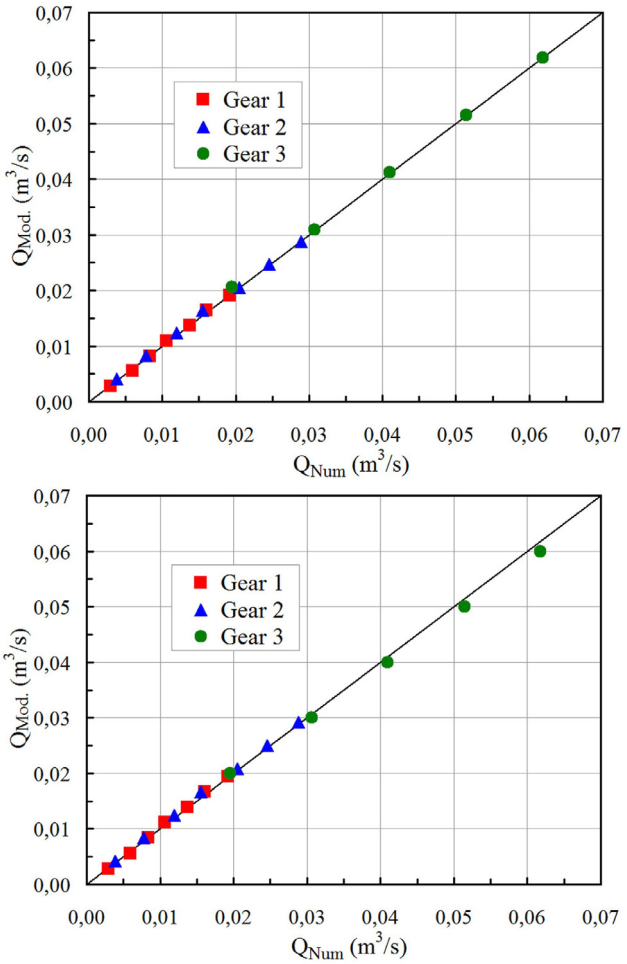


Fig. 7. Comparison of theoretical and numerical volumetric flow rate when using λ estimated from each gear (a) or when using mean value of λ (b).

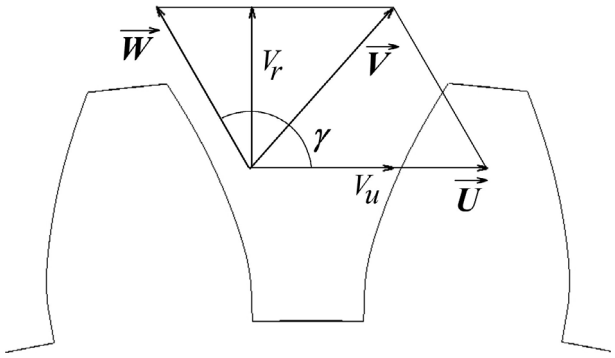


Fig. 8. Triangle of relative velocities

velocity components can be determined as:

$$V_{u2} = U_2 + W_2\cos(\gamma_2) \tag{9a}$$
$$V_{r2} = W_2\sin(\gamma_2) \tag{9b}$$

where $\gamma = \pi/2+$ pressure angle on outside diameter.

In Equation (9b), the velocity radial component can be estimated by using the volumetric flow rate and (8) is

https://doi.org/10.1051/meca/2012028 Published online by Cambridge University Press

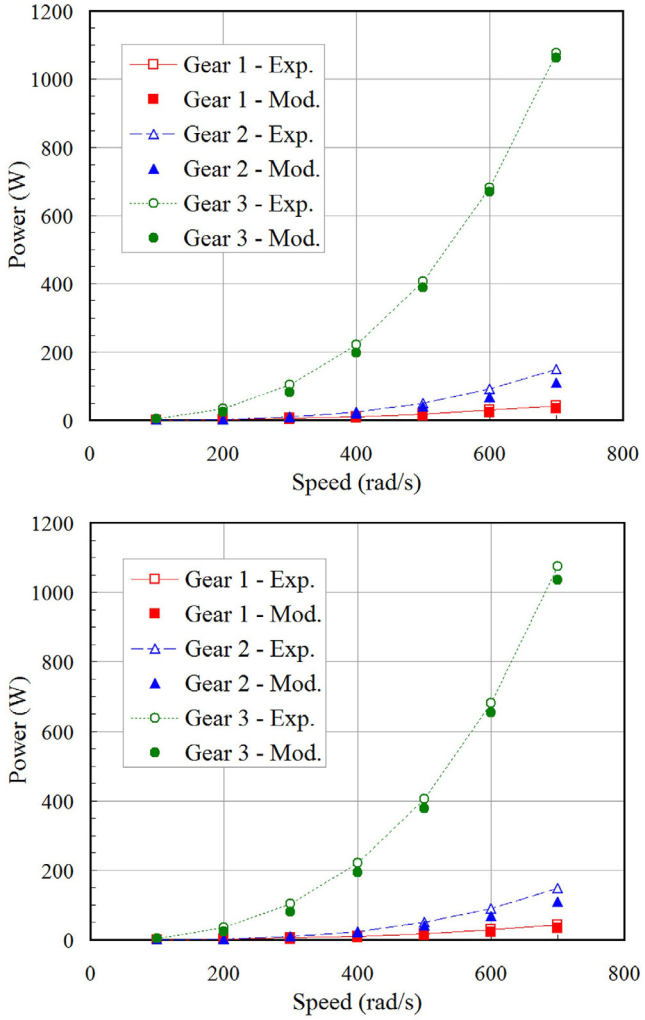


Fig. 9. Windage power loss when using λ estimated from each gear (a) or when using mean value of λ (b).

written as:

$$\mathrm{WPL} = \rho\, Q U_2 \left(U_2 + \frac{Q}{S_2 \tan(\gamma_2)} \right) \qquad (10)$$

where Q is the volumetric flow rate passing through the outlet section area at the exit (radius r_2). Finally the formulation (10) is able to estimate the contribution of teeth on total windage power loss. The dissipation due to viscous effects on gear sides is not considered in the latter formulation and thus is estimated using Diab et al. formulation [5] where both laminar and turbulent regions are involved.

As shown in Figure 9a, when using the value of λ for each gear (5.07×10^{-3} m, 5.05×10^{-3} m, 5.30×10^{-3} m for gears #1, #2, and #3 respectively), the corresponding results are close to the experimental measurements with relative deviations lower than 4% for gear #3 generating the most important loss. More important discrepancies are noticed for the two other gears but WPL are less significant in these cases. It is also noticed that the WPL which is predicted by the model remains lower than the one reached numerically whatever the gear. Once again, when $\overline{\lambda}$ is used to quantify volumetric flow rate through formula (10) more important relative-error is noticed for gear #3 (Fig. 9b) without exceeding 7%. Furthermore the predictions reached for gear #1 and #2 are slightly better since $\overline{\lambda}$ is nearly 2% higher than the two individual values. Another interest of the proposed formula is that it points to a cubic dependency between the WPL generated by the teeth and Ω. Based on the classic results of discs rotating in a fluid [15], the complementary losses associated with the blanks are found to be proportional to $\Omega^{2.8}$ which indicates that the total dissipation is likely to be proportional to Ω^n with $2.8 \leq n \leq 3.0$ in agreement with the empirical equations in the literature [1–5]. Finally, the comparisons with the experimental and numerical values confirm that the contributions of friction at the walls on WPL are of secondary importance compared with the volumetric or pumping effects.

5 Conclusion and discussion

This paper shows that volumetric flow rate has an important role on windage power losses. From the observations of numerical predictions it appears that the former parameter can be related in a simplified point of view to both the tooth height, the number of teeth, the face width and the rotational speed. A formulation of the ejected volumetric flow rate is at first proposed by introducing a coefficient λ. A good agreement is noticed when this coefficient is evaluated for each gear. Then an analogy with turbomachinery is used for building WPL model using the previous model of ejected volumetric flow rate. Power losses predicted by the model are close to the experimental data. It is however noticed that the quality of the predictions depends on the evaluation of coefficient λ: a used mean value of this parameter in the model induces a slight discrepancy of the estimation. It should be noted also that the geometrical characteristic values (e.g. module and face width) in Table 1 are close so that the model which is proposed here would not be appropriate to other gears whose characteristics are far from these values. Further investigations are thus necessary to propose a formulation of λ depending on gear characteristics.

References

[1] N.E. Anderson, S.H. Loewenthal, Effect of geometry and operating conditions on spur gears system power loss, ASME J. Mech. Des. 130 (1981) 151–159

[2] D.P. Townsend, Duddley's gear handbook, New York McGraw-Hill, 1992

[3] P.H. Dawson, Windage loss in larger high-speed gears, Proc. Inst. Mech. Eng. 198 (1984) 51–59

[4] P.H. Dawson, High-speed gear windage, GEC Review 4 (1988) 164–167

https://doi.org/10.1051/meca/2012028 Published online by Cambridge University Press

[5] Y. Diab, F. Ville, P. Velex, C. Changenet, Windage losses in high speed gears – preliminary experimental and theoretical results, ASME J. Mech. Des. 126 (2004) 903–908
[6] S. Seetharaman, A. Kahraman, Load-independent spin power losses of a spur gear pair: model formulation, ASME J. Tribol. 131 (2009) 1–11
[7] K. Al-Shibl, K. Simmons, C.N. Eastwick, Modelling windage power loss from an enclosed spur gear, Proc. Inst. Mech. Eng. 221 A (2007) 331–341
[8] S. Rapley, C.N. Eastwick, K. Simmons, The application of CFD to model windage power loss from a spiral bevel gear, in GT2007, ASME Turbo Expo 2007: Power for Land, Sea and Air, Montreal, 2007, pp. GT2007–27879
[9] M.J. Hill, R.F. Kunz, R.W. Noack, L.N. Long, P.J. Morris, R.F. Handschuh, Application and Validation of Unstructured Overset CFD Technology for Rotorcraft Gearbox Windage Aerodynamics Simulation, in 64th Annual Forum of the American Helicopter Society, 2008
[10] Y. Marchesse, C. Changenet, F. Ville, P. Velex, Investigations on CFD simulations for predicting windage power losses in spur gears, ASME J. Mech. Design 133 (2011) 7
[11] Y. Marchesse, C. Changenet, F. Ville, P. Velex, Influence of tooth geometry on windage power losses in spur gears, in Int. Conf. on Gears, Garching Germany, 2010
[12] J.H. Ferziger, M. Periæ, Computational methods for fluid dynamics, 3rd edition, Springer-Verlag,Germany, 2002
[13] F.R. Menter, Two-equation eddy-viscosity turbulence models for engineering applications, A.I.A.A. J. 32 (1994) 1598–1605
[14] S.L. Dixon, Fluid mechanics and thermodynamics of turbomachinery, 4th edition, Butterworth Heinemann, 1998, p. 321
[15] T. von Kármán, Über laminare und turbulente Reibung. Z. f. a. M. M., Bd. 1, Heft 4 (Aug. 1921) 233–252

https://doi.org/10.1051/meca/2012028 Published online by Cambridge University Press